Field Crops Research 318 (2024) 109545

Contents lists available at ScienceDirect

Field Crops Research

journal homepage: www.elsevier.com/locate/fcr

Optimizing nitrogen rates for winter wheat using in-season crop N status indicators

Raffaele Meloni, Eleonora Cordero, Luca Capo, Amedeo Reyneri, Dario Sacco, Massimo Blandino *

Department of Agricultural, Forest and Food Sciences, University of Turin, Largo Braccini 2, Grugliasco, Italy

ARTICLE INFO

Keywords:
Precision agriculture
Site-specific N management
Vegetation indices
Crop Yield prediction
Grain protein content

ABSTRACT

Conventionally, split nitrogen (N) applications at tillering and stem elongation enhance winter wheat yield, protein content, and nitrogen use efficiency. Vegetation indices, such as the Normalized Difference Vegetation Index (NDVI), Normalized Difference Red Edge index (NDRE), and leaf chlorophyll content (LCC) can be used as crop N status indicators (CNSIs) to easily underline the N deficiency. The aim of this study, conducted across 4 growing seasons in North-West Italy, was to create a model for regulating wheat fertilization rates and improve crop yield. The model relies on CNSIs measurements collected during the initial stages of stem elongation, aiming to achieve predetermined yield targets. In each year, the experimental design was a factorial combination of four N rates (0, 33, 66, and 99 kg N ha^{-1}) at tillering and five at stem elongations (0, 33, 66, 99 and 132 kg N ha^{-1}). The Aubusson cultivar, characterized by intermediate yield potential and protein content, was used to calibrate and validate the model in a 3-year trial (2018–2020), while the model was also applied to cv LG Ayrton (high yield potential) and Izalco (high protein content) in the 2020–21 season. Yield and protein content trends in function of N rate were parabolic or sigmoidal respectively and both tillering and stem elongation rate contributed to increase the grain yield and protein content. Furthermore, the significant interaction between tillering and stem elongation fertilization on grain yield suggested the possibility of correcting the N deficiency after tillering fertilization with a further application. A calibration function for a variable rate application was established related to the CNSIs; all of them were good predictors but NDRE showed a higher overall correlation ($R^2 = 0.479$) with grain yield than NDVI ($R^2 = 0.461$) or the LCC values ($R^2 = 0.236$) considering all the 3 years of experiments. The model's intercept was reduced according to the decrease in the grain yield goal. The model's validation was accomplished by comparing the outcomes predicted by the model yields with the measured. The yield's Root Mean Square Error (RMSE) values were low for cv. Aubusson (0.85, on average) in all 3 years, while the RMSE was higher in 2021 for LG Ayrton (1.90) and Izalco (1.35), in a production situation with a higher yield potential. The results suggest that the topdressing N fertilization rate could be accurately determined from measured CNSI values for a site-specific N fertilization management, but they also highlight the requirement of a model adaptation for different genotypes and environments.

1. Introduction

Wheat is the first world crop per cultivated surface worldwide (219 million hectares, Faostat 2020) and the growing area has been constant since 2000. However, the grain yield is constantly growing (+21 %), due to introducing of new cultivars with a higher input-use efficiency (Tabak et al., 2020).

In addition to the genotype potential, nitrogen (N) fertilization plays a crucial role. The lack of this macronutrient is the most limiting factor for canopy development and for maintaining the stay green, and thus for

Abbreviations: ANOVA, analysis of variance; CEC, cation-exchange capacity; CNSI, crop nitrogen status indicator; Cv, cultivar; GDDs, growing degree days; GLM, general linear model; GPC, grain protein content; GS, growth stage; LCC, leaf chlorophyll content; N, nitrogen; NDRE, normalized difference red-edge index; NDVI, normalized difference vegetation index; NUE, nitrogen use efficiency; PA, precision agriculture; REGWF, Ryan-Einot-Gabriel-Welsh F test; MAE, Mean Absolute Error; RMSE, Root Mean Square Error; VI, vegetation index; VRA, variable rate application.

* Corresponding author.
E-mail address: massimo.blandino@unito.it (M. Blandino).

https://doi.org/10.1016/j.fcr.2024.109545
Received 3 January 2024; Received in revised form 27 June 2024; Accepted 11 August 2024
Available online 7 September 2024

the overall photosynthesis potential (Malhi et al., 2001).

N fertilizers are the most applied agricultural fertilizers throughout the world, with an agricultural use of 113 million tonnes in 2020 (FAOSTAT). The distribution of N based fertilizers increased during the 20th century to support the growing wheat yield resulting from the introduction of new genotypes by breeders during the Green Revolution (Hirel et al., 2007). Each cultivar requires a certain amount of N in different production situations to maximize the yield and to be economically sustainable, which involves maximizing the Nitrogen Use Efficiency (NUE) (Hawkesford and Riche, 2020). Moreover, the availability of N in the field is not constant, and N losses through volatilization, denitrification, runoff and leaching usually occur, due to the high mobility of N and the application of a single uniform N rate (Montemurro, 2009). An additional unrequired fertilizer application does not increase grain yield (Fowler, 2003), and NUE can decrease to a great extent with severe environmental losses (Hawkesford, 2014).

In order to enhance NUE and reduce losses, N should be applied according to the increasing need of wheat in the different growth stages (GS). A split N distribution with readily available forms, such as nitrate or ammonium fertilizers, allows to maximize the grain yield. Compared to a single application of the same fertilizers, this solution enhances the nutrient efficiency and reduces the risk of environmental pollution of this nutrient, which is mainly related to high spring rainfall (Fang et al., 2006). In temperate winter wheat production areas, N is generally split between tillering (GS 22–24, according to Zadoks et al., (1974)) and stem elongation (GS 31–34).

As far as the yield component is concerned, the tillering fertilization is aimed at increasing fertile tillers and the number of ears per surface unit. The aim of stem elongation fertilization is to increase the number of fertile spikelets per head and the kernel dimension (Schulz et al., 2015). A third late fertilization could be performed, from booting to flowering, to improve the grain protein content (GPC). This technique is typical for high protein cultivars (cv), for which the supply chain rewards the achievement of a certain quality threshold, but generally does not result in a further grain yield gain in Mediterranean growing areas (Landolfi et al., 2021). Compared to the use of slow release or controlled fertilizers, a split application allows the total N rate supplied to the crop to be conveniently modulated according to the rainfall and the potential leaching recorded in the spring, before the stem elongation stage (Grant et al., 2012). N fertilization at the stem elongation stage of wheat typically involves higher quantities than at tillering, due to the increasing N requirements in this growing stage. According to Sieling and Kage (2021), fertilizing at stem elongation enhances NUE and is crucial for achieving optimal wheat yield performance. Thus, a careful spatial management applied at this GS could optimize the yield and quality (GPC) and reduce N pollution. After the tillering N application, a N deficiency can be detected in function of soil coverage (number of leaves and stem produced) and leaf colour (yellowing) (Prystupa et al., 2003). Properly sensors can be used to investigate and identify deficient areas within a field, quantify and correct the N deficiency to obtain the specific yield target, intended as the production level that a specific field and variety can reach in a certain year.

Precision agriculture (PA) involves the use of several techniques to attain a better agronomic input management (Diacono et al., 2013). A Variable Rate Application (VRA) of N is a site-specific management procedure that is adopted to reduce over- and under- fertilization and improve a farmer's income by allocating N in the best place at the best time (Diacono et al., 2013). Thus, N distribution can be performed in function of the field variability and whenever the yield of crops needs to be maximized, NUE to be improved, and pollution to be reduced. In addition to the use of indices based on the previous year's yield or some physical and chemical soil parameters, the different N managements areas can be highlighted by directly monitoring the N status in the crop during the growing season. Different light tissue transmitted instruments, such as Yara N-Tester™ (Yara International ASA, Oslo, Norway) or SPAD 502 (Konica Minolta, Chiyoda, Japan), evaluate the leaf chlorophyll content (LLC), providing an estimation of N content in the leaf (Samborski et al., 2009). Particularly, N Tester is a hand-held instrument which quantify the chlorophyll content as a dimensionless index, which values are comprised between 0 (lowest LCC) to 1000 (highest LCC) by exploiting the leaf red and near infrared light transmittance (Aranguren et al., 2019). However, these measurements well assess the leaf N content but are particularly time-consuming and may not be representative of the variability of the whole field, because only a few plants can be sampled, thus accuracy may be reduced (Fitzgerald et al., 2010). Anyway, previous study shows the reliability of these measurements to detect crop N status and guide N fertilization (Ortuzar-Iragorri., 2018). Crop reflectance measurements (remote and proximal sensing) are enhanced tools, based on Vegetation Indices (VIs) obtained from canopy reflectance. They are useful to frequently evaluate the crop status throughout the growing season (Atzberger et al., 2013), in particular as far as N nutrition and variability within the space and time are concerned (Zhao et al., 2018). Since these measurements are non-destructive, rapid and real-time strongly correlated with plant health, the use of crop reflectance and related Vis are effective decision support tools. In addition, it is efficient and useful for spatial and temporal variability assessments (Mulla, 2013). NDVI (Normalized Difference Vegetation Index) and NDRE (Normalized Difference Red-Edge Index) are two of the most widespread VIs used in agriculture. Both indices are calculated as the normalized ratio of the difference between specific wavebands length reflectance. NDVI (Tucker et al., 1985) concern the normalized difference of the near infrared (NIR) and RED wavebands reflectance, while NDRE (Barnes et al., 2000) concern NIR and Red-Edge wavebands. The former is closely related to the biomass and to soil coverage (Raun et al., 2001), but a saturation effect usually takes place when a high biomass or chlorophyll content is encountered (Jiang et al., 2020). NDVI ranges between −1 to 1 negative values are referred to urbanized area and water, values between 0 and 0.3 referred to bare soil, while starting from 0.3 values are related to crop presence with the highest values indicative of green and dense vegetation (Kaliraj et al., 2024). Conversely, NDRE is more sensitive to the N tissue content, and it can better distinguish the canopy colour, with less influence of the aboveground biomass (Cao et al., 2018). As previous, NDRE fluctuate between −1 and 1, with the same meaning of NDVI, but is more valuable during the latest stages of crop growth because it is less prone to saturation compared to the NDVI (Morlin Carneiro et al., 2020). These crop N status indicators (CNSIs) can be detected by both proximal and remote sensors (Mezera et al., 2021). The first ones are usually active instruments (measurements are independent of light condition), carried by tractor sensors such as Greenseaker® (Trimble Navigation Limited, Sunnyvale, USA) or handheld as Crop Circle or Rapidscan (Holland Scientific, Lincoln, USA) (Colaço and Bramley, 2018). The second ones are mainly represented by passive multispectral cameras, through aerial vehicles or by Earth Observation through satellites. Active sensors have been specifically developed and widely used for precision agriculture applications, with the primary objective of optimizing crop management practices such as fertilization (Gebbers and Adamchuk, 2010).

Studies that have focused on the management of a variable rate of N application, in function of field variability, to maximize crop N uptake and reduce N leaching, have been proposed in the last 10 years (Basso et al., 2011). In the majority of cases, the proposed models exploit an over-fertilized strip for both calibration purposes (Holland and Schepers, 2010) and to apply the system to a real field condition (Franzen et al., 2016). To widely disseminate these solutions, there is interest in providing farmers with an easier to apply seasonal prediction N rate model (Hoefsloot et al., 2012) which detects the N deficiency in function of vegetation indices. Moreover, wheat varieties and pedo-climatic conditions can affect the prediction models, depending on the N content in the plant or VIs, thus resulting in their lower applicability (Vannoppen et al., 2020). In a previous work, carried out on rice (Cordero et al., 2018), a model was calibrated to suggest in-season N fertilization at a key growing stage (panicle initiation), in function of

CNSIs, in order to optimize the grain yield according to the target production goal. In the present study the same approach was applied on wheat.

The aim of this research has been to develop a site-specific crop N management practice for common wheat, which could be applied to different production situations to optimize the crop response to this agronomic practice, and to reduce the effect of spatial and temporal variability. In this study, only the CNSIs collected on crops were applied, without any reference value (over-fertilized plot) or weather data, to optimize N fertilization. A model that can predict the N rate at stem elongation in order to maximize the grain yield was calibrated over 3-year field experiments, considering different CNSIs, obtained from the optical measurement of light transmission through the leaf or canopy reflectance, and was validated by considering an additional growing season and different cvs.

2. Materials and methods

The study was conducted in Moncrivello (45°18'39.4"N 8°03'21.9"E, elevation 237 m) in the Po Plain in North-West Italy, over four growing seasons (2017–18, 2018–19, 2019–20 and 2020–21).

Each year, the experiment involved a completely randomized plots design with the factorial combination of four N rates (0, 33, 66, and 99 kg N ha^{-1}) applied at tillering (GS 23, named N_{23}) with five N rates (0, 33, 66, 99, and 132 kg N ha^{-1}) applied at stem elongation (GS 31, named N_{31}) for a total of 20 combinations.

Plots dimensions were 6.5 ×1.5 m and 5 the replications (blocks) were carried out. Three out of five blocks (randomly chosen) in the 2017–18, 2018–19, and 2019–20 growing seasons were exclusively used to calibrate the N management model. The remaining 2 blocks and the whole 2020–2021 experiment, with another 2 genotypes, were used to check the performances of the model (validation).

The normal agronomic techniques adopted in the growing area were applied. Ammonium nitrate (33.5 % N) was used as the fertilizer. The wheat genotype used for calibration (the 2017–18, 2018–19, and 2019–20 growing seasons) was Aubusson (Limagrain Italia S.p.A., Busseto, PR, Italy), an ordinary bread-making cv that is widely cultivated in the growing area. In 2020–21, in order to extend the model to a wider situation, validation of the model was carried out considering different cvs with different phenotypic traits from Aubusson, such as plant height, leaf colour and habitus. For this reason, LG Ayrton (Limagrain Italia S.p.A.), a recently released, ordinary bread-making variety with a high grain yield potential, and Izalco (Lidea, Massa Finalese, MO, Italy), a high protein cv, were considered in the experiment.

The experiment was carried out in different adjacent fields, according to the crop rotation normally applied in the growing area. The previous crop in all the growing seasons was maize, and the fields were ploughed each year, incorporating the residues into the soil. Potassium chloride (60 %) was applied at a rate of 78 kg ha^{-1} of potassium before sowing. No phosphate fertilizer was applied in any of the growing seasons. Planting was conducted in 12 cm wide rows at a seeding rate of 450 seeds m^{-2} in the end of October or beginning of November.

A chemical weed control was carried out with Pinoxaden 3.03 % + Clodinafop-propargyl 3.03 % + Florasulam 0.76 % + Cloquintocet-mexyl 0.76 % (Traxos One®, Syngenta Italia S.p.A., Milano, Italy) at the end of tillering. In order to control foliar and head diseases, the plots were treated with a mixture of a strobilurin and a carboxamide fungicide (Priaxor®, BASF Agricultural Solutions, Lugo (RA) Italy, pyraclostrobin 150 g ha^{-1} and fluxapyroxad 75 g ha^{-1}) at stem elongation (GS 33), and with a mixture of a triazole fungicide (prothioconazole and tebuconazole by Prosaro®, Bayer Cropscience, Milano, Italy), applied at 0.100 kg ha^{-1} of each Active Ingredient (AI) at flowering (GS 62).

The sowing, fertilization, and harvest dates are reported in Table S1, together with the dates of the main growth stages. The soils were sampled at a depth of 0.30 m each growing season at the tillering stage (GS 23), after the winter season and just before the first N fertilization, using Eijkelkamp cylindrical augers. The main physical and chemical parameters of the experiment sites are reported in Table S2. The soil texture in 2018 and 2020 was loam, while it was silty loam in 2019 and 2021. Overall, the soils in the considered area present a generally low N content (<1 %), due to high N leaching in function of the soil texture and the medium-high winter rainfall. During the four-year experiment, N availability was medium-low in 2019 and 2021, because the applied N had been probably poorly washed away as a consequence of the limited rainfall during the winter and spring months. Conversely, medium-high rainfalls might have caused a higher N leaching in 2018 and 2020, thereby reducing the N soil content.

2.1. Field measurements

Three different CNSIs were recorded at the beginning of stem elongation (GS 31) and at milky ripening (GS 75): NDVI and NDRE, using the active hand-held sensors, GreenSeeker™® and RapidSCAN® CS-45, respectively, and the LCC of the top leaf using an hand-held N-Tester™ reader. Greenseaker and Rapidscan instruments collect the reflectance of a self-emitted light source in certain wavelength to calculate the CNSI as follows:

$$\mathrm{NDVI} = \frac{NIR - RED}{NIR + RED} = \frac{770\ nm - 660\ nm}{770\ nm + 660\ nm}$$

$$\mathrm{NDRE} = \frac{NIR - REDEDGE}{NIR + REDEDGE} = \frac{780\ nm - 730\ nm}{780\ nm + 730\ nm}$$

The light emitted by the sensors modulated polychromatic lamp differs from the environmental light for frequency and amplitude. In this way these sensors collect only their own reflectance with optical filtration, and they do not require calibration (Jiang et al., 2020).

The NDVI and NDRE measurements were performed holding the instruments 0.5 m above the canopy to collect indices from an approximately 0.3 wide biomass walking for the entire length of the plot. These sensors scan the crop about 4 time per second and then average all the value for finally store them in their own memory. Commonly, around 20 measurements are automatically taken by the instruments for each plot to have the final value, processed by their own internal software.

The LCC was measured on 30 top unfolded leaves per plot using the N-Tester. This measures the light transmitted by a plant leaf at two different wavelengths to give back an index (Arregui et al., 2006):

$$\mathrm{LCC} = \frac{RED\ (leaf)}{INFRARED\ (leaf)} - \frac{RED\ (environmental)}{INFRARED\ (environmental)} = \frac{650\ nm\ (leaf)}{960\ nm\ (leaf)} - \frac{650\ nm\ (environmental)}{960\ nm\ (environmental)}$$

The environmental light is collected by the instruments clipping without leaf on the sensor at the beginning of the surveys and is useful for the calibration. After clipping 30 leaf the instrument automatically avoids the outliers, average the values and shows the LCC index.

2.2. Grain yield and quality

The plots were harvested using a Walter Wintersteiger cereal plot combine harvester. Grain moisture was analyzed using a Dickey-John GAC2100 grain analyzer (Dickey-John Corp., Auburn, IL, USA), according to the supplied program and after a validation with reference materials. The grain yield results were adjusted to a 13 % moisture content. The harvested grains were mixed thoroughly, and representative sub-samples (500 g) were ground to whole-meal using a laboratory centrifugal mill equipped with a 1 mm sieve (Model ZM-200, Retsch, Haan, Germany). The GPC (N * 5.7, dry weight, AACC method 39-10.01) was determined by means of an NIR System Model 6500 (FOSS-NIR-Systems, Laurel, MD, US).

2.3. Data analysis

The normal distribution and homogeneity of variances were verified by performing the Kolmogorov–Smirnov normality test and the Levene test, respectively. A three-way (N_{23}, N_{31}, Year) analysis of variance (ANOVA) was performed to compare the grain yield, GPC, and CNSIs recorded at different GS, using a completely randomized block design, in which the N_{23} and N_{31} applications, the year, and the interaction between these factors were the independent variables. Multiple comparison tests were performed, according to the Ryan–Einot–Gabriel–Welsh F (REGW-F) method, on the treatment means (p-value<0.05). Moreover, the impact of each factor and their interaction on the total variability of different variables were calculated as the ratio of the variance of each factor, or their interaction, on the total variance of ANOVA. Simple correlation coefficients were obtained for the N rates, CNSI, grain yield, and protein content relative to each other, by splitting the 2017–18, 2018–19, and 2019–20 growing season data sets, to investigate the capability of different VIs to determine the grain yield and GPC. SPSS for Windows, Version 28.0, (SPSS Inc., Chicago, USA), was used for these statistical analyses.

The N model was calibrated starting from the parameters and results obtained from 3 randomly chosen blocks of field experiments pertaining to the 2017–18, 2018–19 and 2019–20 growing seasons on the Aubusson cv. The 2 remaining blocks and the whole 2020–21 experiment were used to validate the model. The N prediction model was set up using R software, version, Version 4.2.1 (R development Core Team, 2016), and according to the procedure described in detail in Cordero et al. (2018), with a few modifications, related to the different application timings of N, which do not consider a pre-sowing fertilization on wheat in comparison to rice, according to the conventional practices of the growing area.

A General Linear Model (GLM) was used to explain the grain yield as a function of N_{23}, N_{31} and the interaction between factors and the slope of the covariates.

$$Yield = \gamma_1 \bullet N_{23} + \gamma_2 \bullet N_{23}^2 + \gamma_3 \bullet N_{31} + \gamma_4 \bullet N_{31}^2 + \gamma_5 \bullet N_{23} \bullet N_{31} \quad (1)$$

where γ stands for the slopes of the covariates, N_{23} and N_{31} are the N supplied at tillering and stem elongation, respectively, and N_{23}*N_{31} represents their interaction.

In order to predict N_{31} to maximize the grain yield as a function of N_{23}, a partial derivative was applied, in function of N_{31}, and set equal to 0. Thus, the resulting model formula was:

$$N_{31} = \frac{(-\gamma_3 - \gamma_5 \bullet N_{23})}{2\ \gamma_4} \quad (2)$$

where N_{31} is the N supplied at stem elongation, γ stands for the slopes of the covariates, and N_{23} is the N applied at tillering. Eq. 2 shows N_{31} as a function of N_{23}, but it becomes meaningless if the interaction between the factors is not significant.

Eq. 1 can be rewritten by replacing N_{23} with the CNSI values, because they are able to accurately describe the effects of tillering fertilization:

$$Yield = \gamma_1 \bullet N_{31} + \gamma_2 \bullet N_{31}^2 + \gamma_3 \bullet CNSI + \gamma_4 \bullet CNSI^2 + \gamma_5 \bullet N_{31} \bullet CNSI \quad (3)$$

Applying a first-order partial derivative to the previous Eq. [3] with respect to N_{31}, and setting it equal to 0 allows the N rate [5] that needs to be applied to maximize the grain yield for each recorded CNSI [4]:

$$Yield = \gamma_1 + 2\gamma_2 \bullet N_{31} + \gamma_5 \bullet CNSI \quad (4)$$

$$N_{31} = \frac{(-\gamma_1 - \gamma_5 \bullet CNSI)}{2\ \gamma_2} \quad (5)$$

Reduction factors of 1 %, 5 %, 10 % and 15 % (99 %, 95 %, 90 % and 85 % of the maximum yield, respectively) were applied to maximum grain yield in order to evaluate how the N demand decreases if the yield goal is lower than the highest goal due to the annual meteorological trends, field fertility and other agronomic conditions. Therefore, the model was again calibrated for each reduced grain yield.

Subsequently, a validation was performed. The function model, developed on 3 blocks of Aubusson cv, was applied to the remaining 2 blocks in the 2017–18, 2018–19 and 2019–20 growing seasons. The grain yield estimation, starting from the CNSI at GS 31, and N_{31} that was applied in each plot, was compared with the real measured yield in each plot for each year. A correlation analysis was performed, and the Mean Absolute Error (MAE) and the Root Mean Square Error (RMSE) were calculated. Finally, the same analysis was carried out with data collected from experiments carried out with cv LG Ayrton and cv Izalco in the 2020–21 growing season.

3. Results

3.1. Weather conditions

The four growing seasons showed different meteorological trends, as far as both rainfall and temperature (expressed as growing degree days, GDDs) are concerned (Table 1). Overall, the 2019–20 growing season had a higher total rainfall (830 mm) than 2017–18 (622 mm), 2018–19 (535 mm) and 2020–21 (428 mm). High rainfall occurred in 2019–20 above all in November and December, leading to a probably higher N leaching at the end of winter, which decreased the N content in the soil at the beginning of spring. Rainfall was particularly limited during the winter period in the 2020–21 growing season, but also from tillering (March) to the end of the stem elongation stages (April). Instead, rainfall was well distributed over time from tillering (March) to the end of ripening stage (June) in 2018, 2019 and 2020, with similar rain amounts for the three years. Overall, the temperatures were similar in all the considered growing seasons. However, it is worth noting that April 2021 was cooler than usual: additionally, rainfall was particularly low, and this led to a reduced disease attack.

3.2. Response of wheat yield and protein content to different N rates

The wheat yields followed a parabolic trend for each considered year as a function of the total N supply ($N_{23} + N_{31}$) (Fig. 1). As expected, the maximum yield was influenced by the different weather conditions, which in turn affected the N uptake. Starting from the N rate-yield curve equations, the highest wheat yield was obtained for 282, 234 and 232 kg N ha^{-1} for 2018, 2019 and 2020, respectively: additional N rates did not lead to any further yield increase. However, from 198 kg N ha^{-1} onwards, the increases were very low, and the grain yields at that rate were 8.5, 6.8, and 9.0 Mg ha^{-1} for 2018, 2019, and 2020, respectively. Conversely, GPC, in function of the N rates, showed a sigmoidal trend. The minimum was not detected in combination with the absence of N fertilization, but it was recorded for the distribution of 33 or 66 kg N ha^{-1} at GS 23 (Fig. 1). On the other hand, a maximum concentration was not detectable and there were clear higher marginal increases compared to the yield for a high N supply.

The N fertilization at both GS 23 and GS 31 had significant effects on the grain yield and GPC (Table 2). Yield was mainly affected by the N_{31} rate (36 % of the total variance), although a high contribution (25 %) came from the N_{23} application. On the other hand, GPC was mainly related to the N_{31} application (64 % of explained variance). Each increase in the N rate at GS 31, from 0 to 132 kg N ha^{-1}, resulted in a significant and linear increase in GPC, while the supply of 33 kg N ha^{-1} at GS 23 resulted in a significant reduction of the protein concentration at harvest, compared to 0 kg N ha^{-1}. Higher fertilization rates at GS 23 further increased the GPC, although fertilization at this GS only affected 8 % explained variance of the GPC.

The differences between years were significant for both yield and

Table 1
Monthly rainfall and growing degree days (GDD) from the sowing (November) to the end of the ripening stage (June) for the four growing seasons.

Growing season	2017–18		2018–19		2019–20		2020–21	
Month	Rainfall	GDD[1]	Rainfall	GDD	Rainfall	GDD	Rainfall	GDD
	(mm)	(Σ °Cd^{-1})	(mm)	(Σ °C d^{-1})	(mm)	(Σ °C d^{-1})	(mm)	(Σ °C d^{-1})
November	48	224	124	292	314	249	4	277
December	33	113	11	151	132	193	79	144
January	107	178	6	141	5	168	116	128
February	60	113	43	195	1	229	29	203
March	109	223	17	314	62	285	8	286
April	93	456	116	393	81	414	37	353
May	138	583	178	478	122	579	69	501
June	35	665	40	667	113	624	86	674
Nov–Jun	622	2554	535	2632	830	2741	428	2567
Nov–Feb	248	627	183	779	452	839	229	752
Mar-Jun	374	1927	352	1853	378	1902	200	1815

[1] Accumulated growing degree days for each experiment using a 0°C base value.
Source: Rete Agrometeorologica del Piemonte - Regione Piemonte - Assessorato Agricoltura - Settore Fitosanitario. Sezione di Agrometeorologia. Weather station located in Borgo d'Ale, 3 km far from the experimental site.

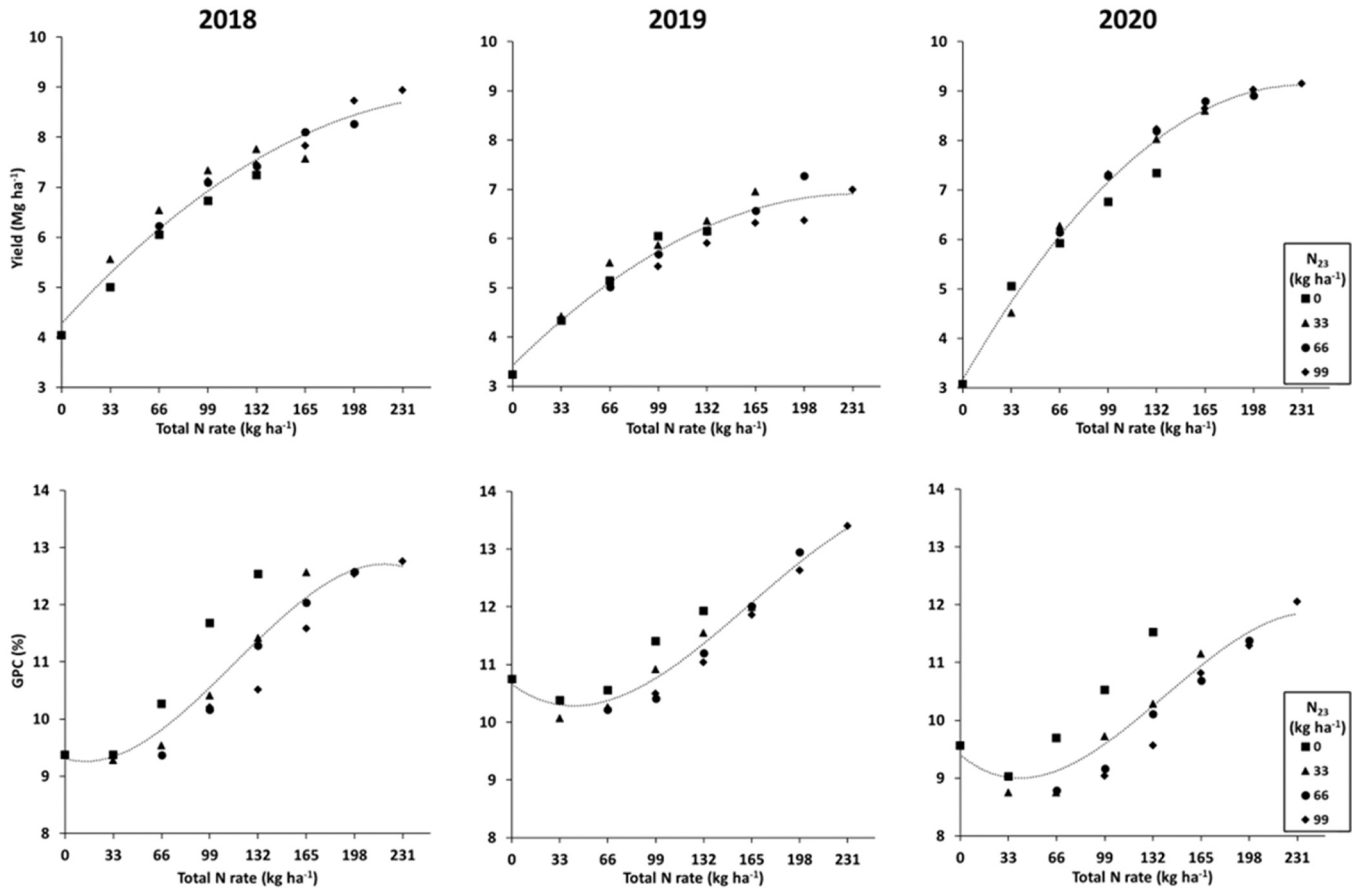

Fig. 1. Grain yield and grain protein content (GPC) response curve as a function of the total nitrogen (N) rates for each growing season. N_{23}: rate of kg N ha^{-1} at the tillering stage. The difference for each total N rates is the amount of N rates at the beginning of the stem elongation stage (GS 31).

GPC. The lowest production and highest protein were measured in 2019, while 2020, which was characterized by higher rainfall - probably connected with high N leaching - resulted in the lowest GPC. The year factor influenced the total variability of the yield and the GPC parameters by 17 %. Similarly, the interaction between N_{23} X N_{31} was statistically significant ($P<0.001$) for both considered parameters, while it only explained 2 % of the total variance. The N_{23} x Year and N_{31} x Year interactions were statistically significant for both the yield and GPC, while N_{23} x N_{31} X Year was only significant for GPC, although its contribution to the overall variance was always < 3 %.

3.3. CNSIs fluctuations in function of different N rates

The CNSIs measured at GS 31 were influenced to a great extent by the previous N fertilization, due to the effect determined by both the plant biomass and the canopy colour (Table 3). The values of all the detected CNSIs (NDVI, NDRE and LCC) rise progressively and significantly for each increasing N rate. The Year factor statistically affected the CNSI values. The highest average NDVI and NDRE values were recorded in 2018, while the highest LCC value was reported for 2019. Conversely, overall, the lowest values of all the CNSIs were detected in 2020. N_{23}

Table 2
Effect of the nitrogen supply application at tillering (N_{23}), beginning of stem elongation (N_{31}), and year on wheat grain yield and grain protein content (GPC).

Factor	Source of variation	Grain yield		GPC	
		(Mg ha^{-1})	Explained variance	(%)	Explained variance
N_{23} (kg ha^{-1})	0	5.5 d	25 %	10.6 c	8 %
	33	6.6 c		10.4 d	
	66	7.1 b		10.8 b	
	99	7.5 a		11.3 a	
	p-value	<0.001		<0.001	
N_{31} (kg ha^{-1})	0	5.2 e	36 %	9.7 e	64 %
	33	6.2 d		9.8 d	
	66	6.8 c		10.7 c	
	99	7.4 b		11.5 b	
	132	7.8 a		12.2 a	
	p-value	<0.001		<0.001	
Year (Y)	2018	7.0 a	17 %	11.0 b	17 %
	2019	5.8 b		11.3 a	
	2020	7.2 a		10.1c	
	p-value	<0.001		<0.001	
N_{23} x N_{31}	*p*-value	<0.001	2 %	<0.001	2 %
N_{23} x Y	*p*-value	<0.001	3 %	0.005	0 %
N_{31} x Y	*p*-value	0.015	1 %	<0.001	1 %
N_{23} x N_{31} x Y	*p*-value	0.964	1 %	<0.001	1 %
Error			15 %		6 %

Means followed by different letters are significantly different for each factor in the REGW-F test. The level of significance (*p*-value) is shown in the table.
[a] The explained variance percentages were calculated as the ratio of the variance of each factor, or their interaction to the total variance of ANOVA.

fertilization explained 56 % of the variance of the LCC value collected at GS 31, while the variability of NDRE was also affected to a great extent by the Year (45 %). The NDVI values recorded at GS 31 were influenced to the same extent by the previous fertilization (N_{23}), the Year, and their interaction.

The CNSI measurements at milky ripening (GS 75) were affected to a great extent by the N_{23} and N_{31} rates, the Year, and their interaction. The N rates at GS 23 were all significantly different from each other for NDVI, while NDRE and above all LCC showed no difference for the low N rate. The N rates applied at GS 31 affected the VIs to a similar extent, although statistical differences were not detected moving from 99 to 132 kg N ha^{-1} for any of the CNSIs. In accordance with the data collected at GS 31, the NDVI values were higher in 2018 than in 2019 or 2020. At GS 75, the Year effect was different for the compared VIs: the highest NDRE and LCC values were detected in 2019, in the growing season with the lowest amount of rainfall, while all the VI values were lower in 2020. Overall, the highest variance components of NDVI and NDRE measured at GS 75 were related to the year factor (47 % and 57 %, respectively), followed by N_{31} and N_{23}. The variability of the chlorophyll foliar content, measured by means of the LCC at GS 75, was mainly explained by the N_{31} rate (46 %), followed by year (32 %), while N_{23} accounted for only 3 % of the total variation. The interaction between N_{23} X N_{31}, N_{23} X Year and N_{31} X Year was always significant, although they always contributed by less than 12 % to the total variance.

3.4. Capability of CNSIs to identify N status and predict Yield and Protein

Correlation matrices were drawn up for each year to determine the relationship between CNSI, grain yield, and GPC in function of the N rate (Table 4). As previously underlined, each CNSI was closely related to the N_{23} rate at GS 31, in particular for NDRE and LCC in 2018 and 2020, while the correlation at GS 75 was significant for all the growing seasons, albeit only for NDVI and NDRE. The VI measurements at GS 75 were closely correlated with N_{31}, but the correlation coefficient increased when the relationship with N_{23} + N_{31} was considered. The total N rate, the sum of N supplied at GS 23 and GS 31, was closely correlated with the grain yield, while GPC was described better by N_{31} alone.

The correlation between CNSI, yield, and GPC was investigated in the same matrices (Table 4). The NDVI and NDRE collected at GS 31 closely matched the same indices measured at ripening, while the LCC values at GS 31 were not correlated with the measurement of this CNSI at GS 75 to any great extent.

The correlation of all the CNSIs with the grain yield was always significant, although the correlation coefficients were always higher at GS 75 than at GS 31. The relationship between CNSI at GS 31 and GPC was only significant for NDRE and the LCC in the 2018 experiment. High correlation coefficients were detected for all the years and for all the VIs measured at GS 75, with the highest values being observed for the chlorophyll content measured by means of the LCC.

3.5. Calibration model used to predict N_{31} to reach a certain yield goal

Fig. 2 reports the calibration results considered to achieve different grain yield goals on the basis of NDVI, NDRE, and LCC. The lines, top to bottom, refer to 1 %, 5 %, 10 %, and 15 % of the maximum yield reduction. All the calibration curves are parallel to each other within the CNSI, while the slope changes slightly between NDVI and NDRE (Eqs. 6 and 7). The different slope value of the LCC function (Eq. 8) is only due to the different scale of this index.

$$99\%yield: \quad N_{31} = -181.313 \bullet NDVI_{31} + 255.462 \tag{6}$$

$$99\%yield: \quad N_{31} = -180.997 \bullet NDRE_{31} + 201.394 \tag{7}$$

$$99\%yield: \quad N_{31} = -0.3196 \bullet LCC_{31} + 312.841 \tag{8}$$

A larger N rate is required for each CNSI to increase the yield from 95 % to 99 % than from 85 % to 90 %. A rate of 150, 157 and 146 kg N ha^{-1} are required to obtain the 99 % of maximum yield for NDVI, NDRE, and LCC values of 0.580, 0.240 and 520, respectively, which represents the average values of the CNSIs over the three years. Only about 65 kg N ha^{-1} are enough to obtain 85 % of the maximum yield. The model shows that when the wheat vigor and/or nutritional status (and the related CNSI values) are increased, the amount of N that needs to be provided at GS 31, in function of the yield goal, is reduced. Therefore, a lower yield target decreases the required N. However, no CNSI values detected at GS 31 allow N_{31} fertilization to be avoided to maximize the yield, thus it can be seen that the crop always requires N fertilization at GS 31 to maximize the yield.

3.6. Model validation

Validation of the model, calibrated in 2018, 2019, and 2020 on Aubusson cv, was performed on other plots of the same variety cultivated in the same period, and considering data collected on different genotypes in the 2020–21 growing season. NDRE collected before the N_{31} application was chosen to validate the model. Indeed, this index was the one most closely correlated with the N rate at GS 31 and with the grain yield over the years, and it is an easier large-scale detectable index than LCC. The yield predicted by the model, on the basis of the NDRE measurements and the applied N_{31} rate, was compared with the one measured in each of the considered production situations. As far as the data collected on cv. Aubusson is concerned (Fig. 3 *A, B, C*), the model overall MAE was about 0.72 Mg ha^{-1} in the 3-growing seasons. The model instead predicted the yield better for each year: on average, a MAE of 0.55 and 0.58 Mg ha^{-1} was recorded for 2018 and 2019, while in 2020 the model underestimated the yield by 1.06 Mg ha^{-1} due to the high yields of this year. The R^2 values were 0.81, 0.77, and 0.92 for 2018, 2019, and 2020, respectively. Furthermore, the RMSE was low

Table 3
Effect of the nitrogen supply application at tillering (N_{23}) and at the beginning of stem elongation (N_{31}), and of the year on the Crop Nitrogen Status Indicators (CNSI)[a] collected at the beginning of stem elongation (GS 31) and at milky ripening (GS 75).

Variable		$NDVI_{31}$	explained variance[b]	$NDRE_{31}$	explained variance	LCC_{31}	explained variance	$NDVI_{75}$	explained variance	$NDRE_{75}$	explained variance	LCC_{75}	explained variance
N_{23} (kg ha^{-1})	0	0.456 d	25%	0.167 d	39%	424 d	56%	0.572 d	9%	0.233 c	12%	514 b	3%
	33	0.577 c		0.232 c		508 c		0.643 c		0.258 bc		502 b	
	66	0.627 b		0.273 b		558 b		0.697 b		0.282 b		530 ab	
	99	0.658 a		0.306 a		593 a		0.747 a		0.316 a		567 a	
	p-value	<0.001		<0.001		<0.001		<0.001		<0.001		<0.001	
N_{31} (kg ha^{-1})	0							0.555 d	28%	0.214 c	19%	383 d	46%
	33							0.637 c		0.242 c		456 c	
	66							0.688 b		0.278 b		560 b	
	99							0.713 a		0.305 ab		600 ab	
	132							0.731 a		0.322 a		643 a	
	p-value							<0.001		<0.001		<0.001	
Year (Y)	2018	0.679 a	22%	0.323 a	45%	532 b	28%	0.720 a	47%	0.315 b	57%	580 a	32%
	2019	0.551 b		0.219 b		569 a		0.669 b		0.326 a		589 a	
	2020	0.508 c		0.193 c		451 c		0.605 c		0.176 c		417 b	
	p-value	<0.001		<0.001		<0.001		<0.001		<0.001		<0.001	
N_{23} x N_{31}	*p*-value							<0.001	2%	0.026	1%	0.023	1%
N_{23} x Y	*p*-value	<0.001	24%	<0.001	10%	<0.001	4%	<0.001	2%	<0.001	2%	<0.001	2%
N_{31} x Y	*p*-value							0.016	3%	<0.001	2%	<0.001	11%
N_{23} x N_{31} X Y	*p*-value							0.939	0%	0.674	1%	0.002	2%
Error			27%		10%		8%		9%		7%		4%

Means followed by different letters were significantly different in the R-E-G-W-F test. The level of significance (*p*-value) is shown in the table.

[a] NDVI, Normalized Difference Vegetation Index; NDRE, Normalized Difference Red Edge index; LCC, leaf chlorophyll content

[b] The explained variance percentages were calculated as the ratio of the variance of each factor, or their interaction, to the total variance of ANOVA.

Table 4
Pearson's correlation coefficient between the Crop Nitrogen Status Indicator (CNSI)[a] detected at the beginning of stem elongation (GS 31) and at milky ripening (GS 75), the grain yield and the Grain Protein Content (GPC) for the 2018, 2019, and 2020 experiments.

Year	Parameter	$NDVI_{31}$	$NDRE_{31}$	LCC_{31}	$NDVI_{75}$	$NDRE_{75}$	LCC_{75}	Grain yield	GPC
2018	N_{23}	0.827***	0.893**	0.899***	0.492***	0.618***	0.197	0.597***	0.272**
	N_{31}				0.642***	0.633***	0.844***	0.634***	0.909***
	N_{23+31}				0.809***	0.880***	0.785***	0.868***	0.882***
	$NDVI_{31}$		0.901***	0.890***	0.473***	0.589***	0.227	0.650***	0.170
	$NDRE_{31}$			0.914***	0.538***	0.623***	0.187	0.643***	0.248*
	LCC_{31}				0.547***	0.632***	0.219	0.647***	0.281**
	$NDVI_{75}$					0.921***	0.840***	0.872***	0.733***
	$NDRE_{75}$						0.800***	0.940***	0.742***
	LCC_{75}							0.817***	0.812***
	Grain yield								0.713***
2019	N_{23}	0.404***	0.614***	0.787***	0.638***	0.648***	0.293*	0.348***	0.337**
	N_{31}				0.510***	0.480***	0.852***	0.630***	0.802***
	N_{23+31}				0.796***	0.779***	0.385**	0.710***	0.838***
	$NDVI_{31}$		0.777***	0.492***	0.544***	0.532***	0.087	0.414***	0.161
	$NDRE_{31}$			0.657***	0.606***	0.567***	0.144	0.453***	0.166
	LCC_{31}				0.513***	0.553***	0.156	0.299*	0.086
	$NDVI_{75}$					0.934***	0.820***	0.847***	0.609***
	$NDRE_{75}$						0.771***	0.788***	0.643***
	LCC_{75}							0.806***	0.738***
	Grain yield								0.610***
2020	N_{23}	0.925***	0.956***	0.973***	0.667***	0.284**	0.162	0.637***	0.188
	N_{31}				0.614***	0.890***	0.909***	0.676***	0.898***
	N_{23+31}				0.895***	0.874***	0.813***	0.926***	0.821***
	$NDVI_{31}$		0.987***	0.967***	0.680***	0.247*	0.120	0.659***	0.101
	$NDRE_{31}$			0.973***	0.688***	0.276**	0.145	0.660***	0.133
	LCC_{31}				0.675***	0.320*	0.131	0.666***	0.145
	$NDVI_{75}$					0.760***	0.658***	0.967***	0.575***
	$NDRE_{75}$						0.913***	0.787***	0.891***
	LCC_{75}							0.716***	0.920***
	Grain yield								0.642***

(*) = correlation significant for p-values ≤ 0.05; (**) = correlation significant for p-values ≤ 0.01; (***) = correlation significant for p-values <0.001. The data reported in the table are Pearson product-moment correlation coefficients.

[a] NDVI, Normalized Difference Vegetation Index; NDRE, Normalized Difference Red Edge index; LCC, leaf chlorophyll content

and comparable for 2018 and 2019 (0.67 and 0.73), while it increased in 2020 (1.15).

As far as the data collected on cv LG Ayrton and cv Izalco in 2021 are concerned (Fig. 3 *D* and *E*), the model underestimated the grain yield for both varieties (MAE of 1.71 and 1.13 Mg ha^{-1} for LG Ayrton and Izalco, respectively). The R^2 values were lower than those detected in the previous years for cv Aubusson, in particular for the Izalco genotype (0.69), while the RMSE values were slightly higher (1.90 and 1.35 for LG Ayrton and Izalco, respectively).

4. Discussion

The data of the present study, which was conducted over 4 growing seasons and involved comparing a large combination of N_{23} and N_{31} fertilization applications, further highlights the key role of N fertilization on wheat yield performance. Moreover, it is clear the importance of defining a rate that can guarantee the target for each production situation, while considering the agronomic, economic, and sustainable aims. Furthermore, the data reported a more marked effect of the N rate on grain quality (e.g. GPC) than the yield, as previously reported for temperate growing areas by Marinaccio et al. (2016) and Litke et al., (2018).

The relationship between N amount and yield was found to be parabolic. The optimum N rate to maximize the yield was 198 kg N ha^{-1}, a value that is comparable with the 180 kg N ha^{-1} observed by Litke et al. (2018) in a trial performed in north Europe on a loam soil with a high organic matter and medium N content. The marginal increases were very low (< of 10 kg of yield per kg of N) for an extra N rate, although the maximum yield was reached according to the proposed curve equation for a total of 282, 234, and 232 kg N ha^{-1} each year. A maximum peak of protein content was not achieved in the research carried out by Litke et al., (2018), although a still high marginal increase was reported for further increases in N rate, similar to observed in our study.

Fertilization at both tillering (N_{23}) and stem elongation (N_{31}), and their interaction, contributed substantially to the wheat yield and GPC. The significant interaction between the N rate on wheat yield is worthy of noting, and it suggests the possibility of correcting an N_{23} rate deficiency with a subsequent N_{31} topdressing fertilization. A split N application could help to satisfy the N demand of wheat during the crop cycle, particularly in the two uptake peak periods (tillering and stem elongation until heading), which are fundamental to maximize the yield components (Ma et al., 2021). N fertilization at both tillering and stem elongation, applied as ammonium nitrate, contributed to the same extent to the final yield. However, according to Marino et al. (2011), GPC is influenced largely by N_{31} fertilization, rather than at the earlier stage (N_{23}), according to the N kernel storage, which is concentrated at the end of the crop cycle. In a previous study, Aranguren et al. (2021) showed no general relationship over the years between CNSI measurements collected at flowering and GPC values under humid Mediterranean conditions. Conversely, the capability of all the CNSIs to predict GPC has been highlighted in this study, but only when detected at the grain ripening stage (GS 75), as a measure of the last N fertilization (N_{31}).

This study clearly points out the capability of CNSIs to indicate the morphological and canopy color differences of crops, as a consequence of their different nutritional status. Quebrajo et al. (2015) reported a high capability of the CNSIs collected by active sensors to investigate the leaf nitrogen content as expression of nutritional status. The different fertilization rates, but also the meteorological trend of each year, with its influence on N leaching and uptake, influenced both the colour and vigor of the crops, and this resulted in CNSI variations strictly related to N deficiency. CNSIs are very sensible at the N fertilization rate applied on wheat and they change according to the N uptake by the plants, with

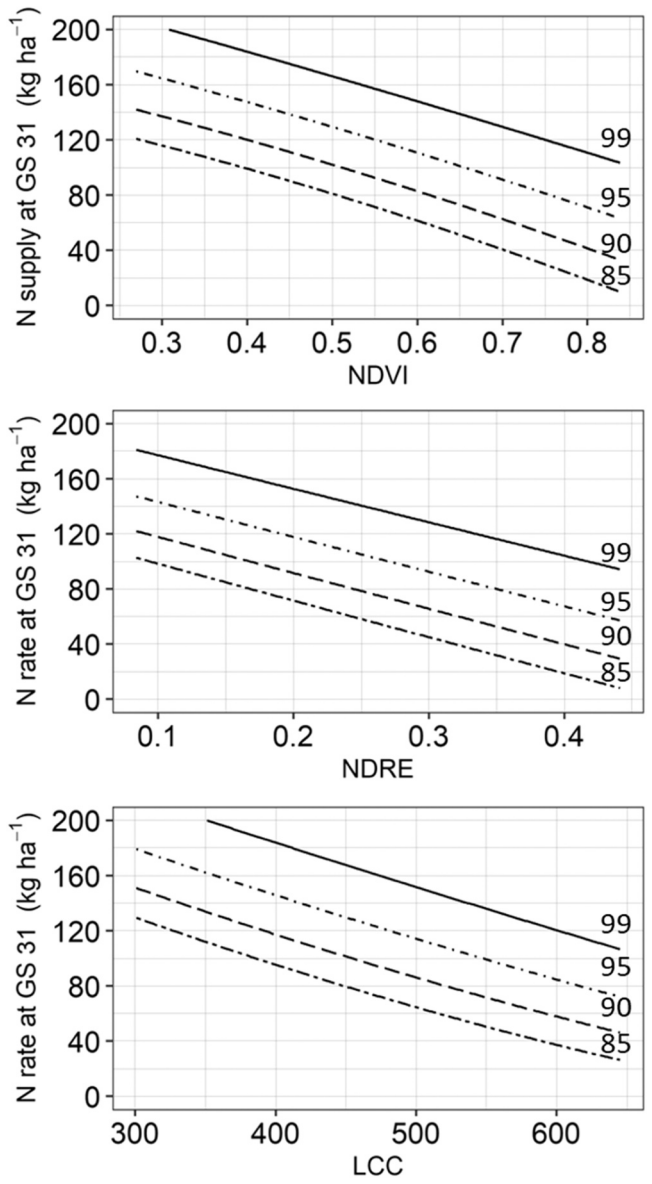

Fig. 2. Calibration functions for the nitrogen (N) rate fertilizer spreading at stem elongation (GS31) as a function of different crop N status indicators (CNSI)[1] and progressively decreasing grain yield goals[2]. [1] NDVI, Normalized Difference Vegetation Index; NDRE, Normalized Difference Red Edge; LCC, leaf chlorophyll content. [2] The solid black line represents the calibration function of each CNSI for 99 % of the maximum grain yield. The dashed black lines moving downwards, represent the calibration functions considered to obtain 95 %, 90 %, and 85 % of the maximum grain yield, respectively.

an increasing precision if only the year data are considered (Li et al., 2010). Plant tissues with N deficiency reflect more light than N-sufficient ones, but usually les slight in the NIR region, which is used for the calculation of the CNSIs in this study (Tremblay et al., 2011). According to these, all the CNSIs in this work were able to point out the nutritional status of the crop at GS 31 related to the N rate applied in an earlier GS. Thus, for all the considered CNSIs, this study has developed predictive models that allowed quantify the optimal N rate at GS 31 according to the grain yield goal. The slope of the models, based on different CNSIs, obtained by considering canopy reflectance (NDVI, NDRE) or leaf transmission (LCC) measured through the N-Tester, were similar, due to the high correlation observed between the VIs measured at GS 31. Practically, lowest values of the CNSIs suggest high N deficiency and require and higher amount of N for the same yield compared to high CNSIs values.

Furthermore, since NDRE showed a higher correlation with N_{31} and yield than NDVI or the LCC, it was considered the most suitable index to develop a prediction model to apply at a large-scale. As also highlighted by Cordero et al. (2018) on rice in the same growing area as that of the present experiment, and then confirmed by Prey and Schmidhalter (2019) on wheat, NDRE shows a better R^2 value than the other CNSIs, related to grain yield. (Wang et al., 2019) reported the same result with a slightly better performance of NDRE compared to NDVI in predicting both yield and crop N status, since this CNSI exploits spectral band related mostly with N concentration in the plants. In another experiment, Quebrajo et al. (2015) reported in wheat R^2 values similar to the ones observed in the present manuscript, without a difference between NDVI and NDRE.

Remote sensing sensors can easily detect NDRE, with a spatial resolution that is 10 or 20 m for free Sentinel-2 imagines (Delwart, 2015), although it could reach 0.5 m with a private satellite service (Anger et al., 2020). In a previous study (Farbo et al., 2022), the correlation between VIs collected by proximal and remote sensors was demonstrated to be very high, thus suggesting the possibility of applying the presented model at a large scale, using satellite data. However, validation of these remote sensors at a territorial level is still necessary. This involves relevant factors such as sensor types, data processing techniques, crop and cultivar characteristics, and integration of multiple data sources for a comprehensive and effective N management in agriculture (Zhang et al., 2024).

Although the LCC measurements showed a significant relationship with the N_{23} rate, this CNSI would not permit a rapid application of the model to a large growing area or to areas with numerous production situations, due to the long time necessary to detect this VI. Although this method would not easily permit the calculation of VRA of N, it could be applied to define the best fertilizer rate to optimize the yield of a whole field, according to the variability over the growing seasons. Furthermore, LCC measurements are closely related to the leaf N content and, for this reason, they are able to provide a more reliable prediction of grain quality, in terms of protein content, than the other measurements. As in this study, Aranguren et al. (2021) found a close correlation of this CNSI, collected in the late GS, with GPC, due to the capability of CNSI to quantify the N flag-leaf content, which moves to the spike during the grain filling period.

The proposed N fertilization strategy is based on the assumption of applying quickly-available N fertilizers, split into different key stages of crop development. This strategy is the most frequent solution applied by farmers in humid temperate growing areas on winter wheat (Zhang et al., 2021). It permits farmers to control the N supply during plant development and according to the seasonal variability of rainfall and the nutritional status of the crop (N deficiency). The first fertilization at tillering (N_{23}) should mainly be defined by farmers in function of the winter rainfall, and the crop status at the end of winter (plant density and vigor), while other agronomic factors, such as the soil fertility, the crop precession, and the tillering capacity of the cv, should also be taken into consideration. Other studies considered the tillering fertilization as fixed and applied VR fertilization at the stem elongation or at heading, due to their higher impact on grain yield and protein content, respectively (Elbl, 2019). However, the use of CNSIs to guide fertilization at this GS could be less useful, since the detected VIs may be less indicative of the availability of N for the crop. In fact, a high interference with soil (low canopy coverage) can mislead the correct fertilization prescription in this GS (Wang et al., 2012). Moreover, the presence of weeds, before their chemical control, can increase the VI values, thus leading to an underestimation of the N that is required. Moreover, a rate of 30–60 kg N ha^{-1} is usually adopted in temperate growing areas at GS 23. Considering the low range of possible N rates, a VR application might not be necessary, above all with the possibility of correcting the N deficiencies or excesses with a further N_{31} application. Furthermore, in fields characterized by a large variability, in terms of soil fertility, the

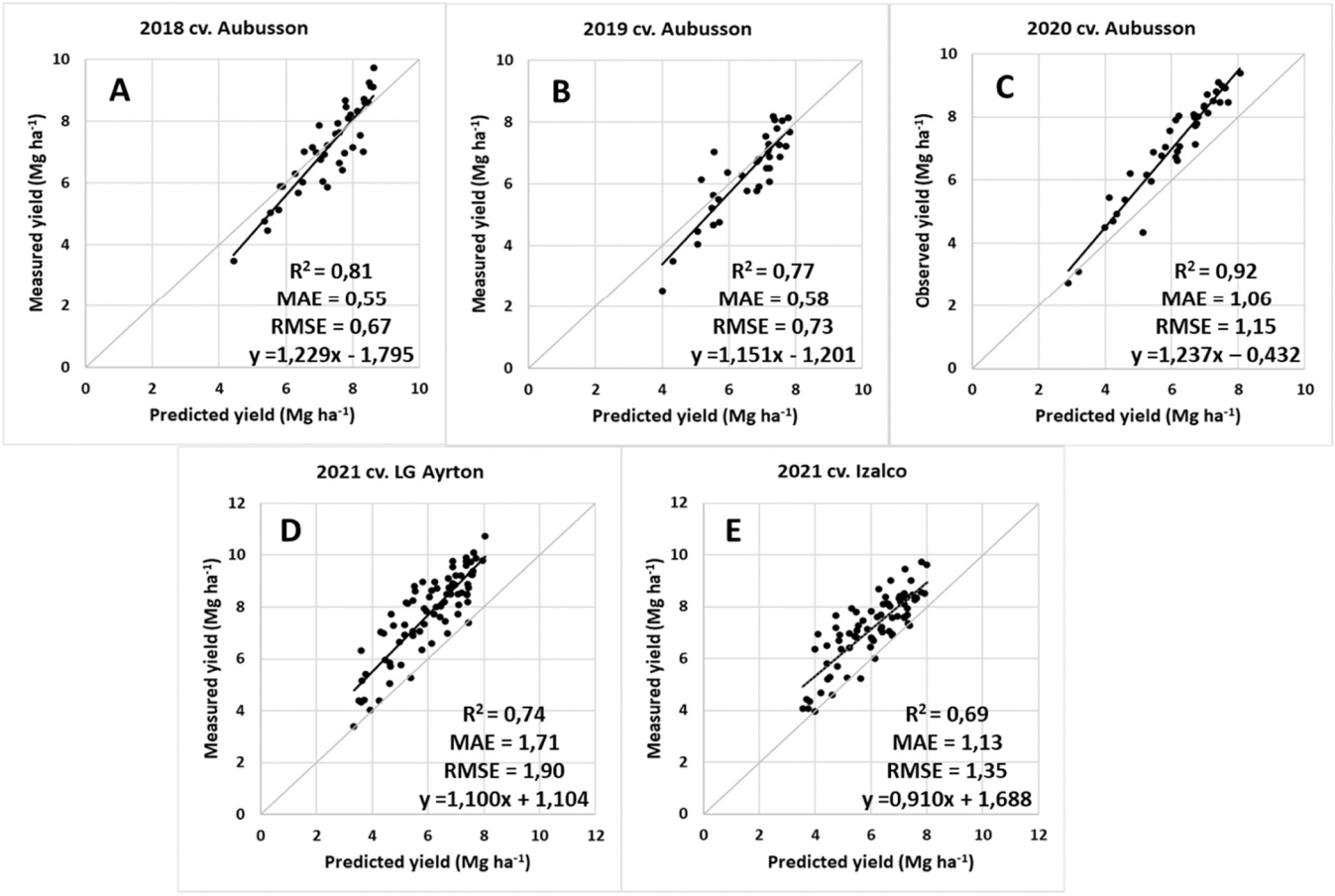

Fig. 3. Relationship between the measured yields and those predicted by the model based on the nitrogen rate at stem elongation (GS31) as a function of the NDRE. Graphs A, B and C compare the yield values predicted by the model vs measured on cv. Aubusson in 2018, 2019, and 2020, respectively. The plots used for calibration are excluded. Graphs D and E compare the yield values predicted by the model vs measured on cv. LG Ayrton and cv. Izalco in 2021.

application of VR in this GS could be based mainly on different approaches from the use of CNSI, such as the use of soil texture (which is closely related to N leaching) or previous year yield maps (Basso et al., 2011).

The developed model permits the second fertilization at the beginning of stem elongation (N_{31}) to be controlled according to the CNSI. This second N application is linked more to the wheat grain yield than N_{23} fertilization, and the nutrient rates are usually higher than at tillering. For these reasons, a careful VR management is more important to avoid the unnecessary spreading of N or a higher lodging in fertile fields, or a lower grain yield and quality due to lower N rate than potentially required (Boulelouah et al., 2022).

The quality of the model was high, according to the R^2 and RMSE calculated between the predicted and observed grain yields. Similar values to those reported in previous studies, carried out using only NDVI detected at GS 31 and weather data (Pennacchi et al., 2022; Gobbo et al., 2022) were found. Moreover, the present model was not calibrated on a reference overfertilized strip, as is usually done to obtain a non-limiting N situation (Colaço and Bramley, 2018). An overfertilized strip allows the maximum CNSIs to be reached and the N rate to be calibrated on the basis of such values. However, an overfertilized strip may be located in a non-representative zone of a field. Consequently, both positive and negative calibration problems can arise, without considering that farmers have to carry out these dedicated operations.

The presented model was applied over the four growing seasons. The obtained data highlight its applicability, with a similar precision, for different growing seasons, although certain abiotic stresses (drought stress and low tillering in 2019) and biotic ones (*Fusarium* head blight attack in 2018) resulted in a clear negative constraint for the grain yield potential (Boulelouah et al., 2022). Yearly yield fluctuations found in this study were in accordance with the meteorological trends which have influenced the agronomic performance in each growing seasons, and they are consistent with the observed average yield in the area. The expected average N uptake, calculated in function of grain yield and N content, was similar between the growing seasons (135, 115 and 128 kg N ha^{-1} in 2018, 2019 and 2020, respectively), since the year with the lowest yield (2019) resulted in the highest GPC. Considering the application of the model in the production situations of the present experiment, the R^2 obtained from the validation carried out in 2019 was the lowest, probably due to the limited rainfall, which resulted in higher N soil availability and plant uptake, together with a lower contribution of the applied fertilizers. Conversely, in 2020, the more abundant rainfall might have increased winter N leaching, thus making the effects of N fertilization on the CNSI and grain yield clearer. The slope of the function of the prediction model highlighted a similarity over the years on the same genotype (cv. Aubusson). Furthermore, in 2018 and 2019, the model tended to overestimate the yield below 7.5 Mg ha^{-1} and to underestimate it for higher level. Besides, the higher yield levels 2020 decreased the accuracy of the model, and resulted in a general underestimation, although the R^2 of the model validation was the highest and the MAE and RMSE were the most consistent. Pennacchi et al. (2022) also reported that the RMSE value showed yearly fluctuations for different wheat yield levels in function of the meteorological data. Appling the model to the datasets obtained in 2021 for different genotypes (cv. Ayrton and Izalco), the R^2 supported the goodness of prediction, although a general yield underestimation was observed. This

underestimation and the higher MAE and RMSE, in addition to the specific conditions of a different growing season, could explain the higher yield potential that characterizes these two recently released cvs, compared to Aubusson, a widely cultivated cv, on which the model was calibrated. Although the validation functions for these genotypes were similar to those observed for Aubusson in 2020, the year with the highest grain yield for this cv, the different canopy colour and plant habits, as well as the variable yield potential of each genotype could imply the need for a calibration process to correctly adapt this model to different wheat categories. This process would need to be defined according to specific traits, such as yield potential, precocity, and the tolerance to biotic and abiotic stress. In particular, the proposed model may require a different calibration, as far as N_{23} and N_{31} plant needs are concerned, for wheat cvs that can be sown at a low seed rate, to exploit their higher tillering ability, such as the recent commercial F1 variety hybrid (Buczek et al., 2017).

Farmers play a key role in choosing the fertilization rate to reach a specific yield goal. With their experience, considering the overall agronomic status of the crop, the economic context (e.g. cost of N fertilizers and the expected kernel price) and that a 100 % yield potential is unachievable (Cordero et al., 2018; Pennacchi et al., 2022), they can enhance the NUE and crop income.

The proposed methodology, unlike the management of fertilization required to reach the yield goal, was not able to return a useful model to manage the N application in order to address bread-making quality. Since Aubusson is an ordinary bread making cv, which only requires a minimum market threshold value of the protein content to be surpassed for it to be commercialized without any qualitative penalty (GPC > 11.5 %; Foca et al., 2007), and without any further premium price for kernels with higher qualitative traits, there is no economic interest in this market category to maximize the GPC. In our experiment, the highest N_{23} rate needed to be supported by at least another 66 kg N ha^{-1} at GS 31 to reach this qualitative threshold in 80 % of the cases. Moreover, regardless of the N_{23} rate, almost all the plots fertilized at stem elongation with 132 kg N ha^{-1} (95 %) reached a higher GPC level than 11.5 %. Furthermore, the relationship between N fertilization management (rate and timing) and GPC is described by a sigmoid curve. The supply of 33 kg N ha^{-1} at GS 23 resulted in a significant reduction of the protein concentration at harvest, compared to 0 kg N ha^{-1}, and this was probably related to a positive effect on the number of spikes per surface unit, which determined a dilution of the available N into a higher sink. This trend differed from that between N and grain yield, which is parabolic, and therefore the strategy to manage the N application at GS 31 to increase the yield, according to the CNSI, did not maximize the GPC. As Hellemans et al. (2018) also reported, the GPC was more closely related to the N fertilization rate at stem elongation than at tillering, while the late season timing, between booting to flowering, could lead to a further important contribute (Blandino et al., 2020). For these reasons, and also considering the weak relationship between CNSI collected at GS 31 and the protein content and the sigmoidal GPC trend in function of N_{23+31}, the proposed model may only be exploited to maximize the grain yield, following the N_{31} rate model suggestion, to obtain a specific yield goal. Elbl, (2019) show that the variable N rate application in open field experiments allow to increase the wheat grain yield without affecting the quality as protein content. The qualitative target, in terms of GPC, is strictly required for improver high protein wheat (GPC >13.5 %, Foca et al., 2007). In temperate growing areas this wheat cvs receive a third late season N fertilization (Blandino et al., 2020). For this reason, a model could be developed to guide this practice at heading in order to optimize and standardize the quality of this market category, starting from VIs detected at the booting stage. Further studies, focusing on defined market categories for which the achievement of a qualitative target is mandatory. It will be necessary to investigate the relationship between CNSIs and GPC, as well as to establish the correct N rate at stem elongation or in a later GS, in order to satisfy the supply chain request by optimizing the N application and producing a further enhancement of NUE.

5. Conclusions

This study has highlighted the possibility of managing the variable N fertilization rate at stem elongation to attain specific yield goals, through the use of such CNSIs as NDRE or NDVI, which are easily obtainable through proximal or remote sensing at the end of the tillering stages. The field experiment carried out over different growing seasons and on different cvs clearly supported the use of the wheat crop as an indicator of N availability in the soil, according to the meteorological trends and the agronomic management practices. Thus, the top-dressing N fertilization rate can be accurately determined by means of a calibration function based on in-season CNSI values. In this way it is possible to avoid N imbalances and to allow a site-specific N fertilization. Moreover, avoiding inserting any further weather or soil parameters into the model the decision support system is easier to apply to a wider production situations and genotypes.

However, the study has highlighted that the different varietal habitus and canopy colour, which could have an impact on the VI values, and, above all, the grain yield potential of different genotypes, could affect N_{31} forecasting to a certain degree. Therefore, the application of the proposed model to different genotypes may require a more detailed adjustment of the calibration, mainly considering the productive response of the crop to N fertilization.

The application of the model with a different distribution of the N rate can be reasoned in term of VR application within the field, by varying N fertilization as a function of spatial and interannual variability or considering the whole fields as single unit and varying the nutrient rate as a function of interannual variability. This simplified option could be necessary in small fields, considered each as a unique homogeneous area, or when a proper equipment for the variable rate application is not available. In order to guarantee a cheaper and faster management of large growing areas, future research have to focus more on the use of CNSIs detected through passive sensors satellite data, as an interesting alternative of to the active sensors considered in the present study.

CRediT authorship contribution statement

Eleonora Cordero: Writing – review & editing, Investigation, Data curation. **Luca Capo:** Investigation, Formal analysis. **Raffaele Meloni:** Writing – original draft, Investigation, Formal analysis, Data curation. **Massimo Blandino:** Writing – review & editing, Visualization, Supervision, Project administration, Methodology, Investigation, Funding acquisition, Formal analysis, Conceptualization. **Amedeo Reyneri:** Supervision, Funding acquisition. **Dario Sacco:** Supervision, Methodology, Investigation, Conceptualization.

Declaration of Competing Interest

The authors declare the following financial interests/personal relationships which may be considered as potential competing interests. Massimo Blandino reports financial support was provided by Piedmont Region. If there are other authors, they declare that they have no known competing financial interests or personal relationships that could have appeared to influence the work reported in this paper

Data Availability

Data will be made available on request.

Acknowledgements

This work was supported by Regione Piemonte (F.E.A.R.S. Rural Development Program 2014–2020), as a part of the TELECER Project. The authors would like to thank all the field and lab technicians who

made valuable contributions to the study, Marguerite Jones and Susana Albarenque for the English and technical editing.

Appendix A. Supporting information

Supplementary data associated with this article can be found in the online version at doi:10.1016/j.fcr.2024.109545.

References

AACC. Approved Methods of the American Association of Cereal Chemists, 2008. 11th Edn.; St. Paul, MN: The Association, 2008; Vol. Methods, 11th ed.

Anger, J., Ehret, T., de Franchis, C., Facciolo, G., 2020. Fast and accurate multi-frame super-resolution of satellite images. ISPRS Ann. Photogramm. Remote Sens. Spat. Inf. Sci. V. -1–2020 57–64. https://doi.org/10.5194/isprs-annals-V-1-2020-57-2020.

Aranguren, M., Castellón, A., Aizpurua, A., 2019. Crop sensor-based in-season nitrogen management of wheat with manure application. Remote Sens 11 (9), 1094. https://doi.org/10.3390/rs11091094.

Aranguren, M., Castellón, A., Aizpurua, A., 2021. Wheat grain protein content under Mediterranean conditions measured with chlorophyll meter. Plants 10, 374. https://doi.org/10.3390/plants10020374.

Arregui, L.M., Lasa, B., Lafarga, A., Irañeta, I., Baroja, E., Quemada, M., 2006. Evaluation of chlorophyll meters as tools for N fertilization in winter wheat under humid Mediterranean conditions. Eur. J. Agron. 24, 140–148. https://doi.org/10.1016/j.eja.2005.05.005.

Atzberger, C., 2013. Advances in remote sensing of agriculture: context description, existing operational monitoring systems and major information needs. Remote Sens 5, 949–981. https://doi.org/10.3390/rs5020949.

Barnes, E.M., Clarke, T.R., Richards, S.E., 2000. Coincident detection of crop water stress, nitrogen status and canopy density using ground based multispectral data. In: Robert, P.C., Rust, R.H. (Eds.), W.E. 504 Precis. Agric. (2010) 11:488–506 123 Larson. Proceedings of 5th International Conference on Precision Agriculture [CDROM], Madison, WI: American Society of Agronomy.

Basso, B., Ritchie, J.T., Cammarano, D., Sartori, L., 2011. A strategic and tactical management approach to select optimal N fertilizer rates for wheat in a spatially variable field. Eur. J. Agron. 35, 215–222. https://doi.org/10.1016/j.eja.2011.06.004.

Blandino, M., Visioli, G., Marando, S., Marti, A., Reyneri, A., 2020. Impact of late-season N fertilisation strategies on the gluten content and composition of high protein wheat grown under humid Mediterranean conditions. J. Cereal Sci. 94, 102995 https://doi.org/10.1016/j.jcs.2020.102995.

Boulelouah, N., Berbache, M., Bedjaoui, H., Selama, N., Rebouh, N., 2022. Influence of nitrogen fertilizer rate on yield, grain quality and nitrogen use efficiency of durum wheat (Triticum durum Desf) under Algerian semiarid conditions. Agriculture 12 (11), 1937. https://doi.org/10.3390/agriculture12111937.

Buczek, J., Jarecki, W., Bobrecka-Jamro, D., 2017. Hybrid wheat response to topdressing and foliar application of nitrogen. J. Elem. 22 (1), 7–20. https://doi.org/10.5601/jelem.2016.21.2.1125.

Cao, Q., Miao, Y., Shen, J., Yuan, F., Cheng, S., Cui, Z., 2018. Evaluating two crop circle active canopy sensors for in-season diagnosis of winter wheat nitrogen status. Agronomy 8, 201. https://doi.org/10.3390/agronomy8100201.

Colaço, A.F., Bramley, R.G.V., 2018. Do crop sensors promote improved nitrogen management in grain crops? Field Crop. Res. 218, 126–140. https://doi.org/10.1016/j.fcr.2018.01.007.

Cordero, E., Moretti, B., Miniotti, E.F., Tenni, D., Beltarre, G., Romani, M., Sacco, D., 2018. Fertilisation strategy and ground sensor measurements to optimise rice yield. Eur. J. Agron. 99, 177–185. https://doi.org/10.1016/j.eja.2018.07.010.

Core Team, R., 2016. R: A language and environment for statistical computing. R Foundation for Statistical Computing. Austria, Vienna.

Delwart, S., 2015. SENTINEL-2 User Handbook. European Space Agency. ⟨https://sentinels.copernicus.eu/web/sentinel/user-guides/document-library/-/asset_publisher/xlslt4309D5h/content/sentinel-2-user-handbook⟩ (Accessed October 10, 2023).

Diacono, M., Rubino, P., Montemurro, F., 2013. Precision nitrogen management of wheat. A review. Agron. Sustain. Dev. 33, 219–241. https://doi.org/10.1007/s13593-012-0111-z.

Elbl, J., 2019. Evaluation of flat and variable rate nitrogen application effect on winter wheat yield on the basis of yield maps. 19th SGEM Int. Multi. Sci. GeoCo. EXPO Proceedings. ⟨https://doi.org/10.5593/sgem2019/2.2/S11.101⟩.

Fang, Q., Yu, Q., Wang, E., Chen, Y., Zhang, G., Wang, J., Li, L., 2006. Soil nitrate accumulation, leaching and crop nitrogen use as influenced by fertilization and irrigation in an intensive wheat–maize double cropping system in the North China Plain. Plant Soil 284, 335–350. https://doi.org/10.1007/s11104-006-0055-7.

Faostat 2020. Crops and livestock products data 2020. ⟨https://www.fao.org/faostat/en/#data/QCL⟩ (Accessed October 10, 2023).

Farbo, A., Meloni, R., Blandino, M., Sarvia, F., Reyneri, A., Borgogno-Mondino, E., 2022. Spectral Measures from Sentinel-2 Imagery vs Ground-Based Data from Rapidscan© Sensor: Performances on Winter Wheat. In: Borgogno-Mondino, E., Zamperlin, P. (Eds.), Geomatics for Green and Digital Transition, Communications in Computer and Information Science. Springer International Publishing, Cham, pp. 211–221. https://doi.org/10.1007/978-3-031-17439-1_15.

Fitzgerald, G., Rodriguez, D., O'Leary, G., 2010. Measuring and predicting canopy nitrogen nutrition in wheat using a spectral index—the canopy chlorophyll content index (CCCI). Field Crop. Res. 116, 318–324. https://doi.org/10.1016/j.fcr.2010.01.010.

Foca, G., Ulrici, A., Corbellini, M., Pagani, M.A., Lucisano, M., Franchini, G.C., Tassi, L., 2007. Reproducibility of the Italian ISQ method for quality classification of bread wheats: an evaluation by expert assessors. J. Sci. Food Agric. 87, 839–846. https://doi.org/10.1002/jsfa.2785.

Fowler, D.B., 2003. Crop nitrogen demand and grain protein concentration of spring and winter wheat. Agron. J. 95, 260–265. https://doi.org/10.2134/agronj2003.0260.

Franzen, D., Kitchen, N., Holland, K., Schepers, J., Raun, W., 2016. Algorithms for in-season nutrient management in cereals. Agron. J. 108 (5), 1775–1781. https://doi.org/10.2134/agronj2016.01.0041.

Gebbers, R., Adamchuk, V.I., 2010. Precision agriculture and food security. Science 327 (5967), 828–831. https://doi.org/10.1126/science.1183899.

Gobbo, S., De Antoni Migliorati, M., Ferrise, R., Morari, F., Furlan, L., Sartori, L., 2022. Evaluation of different crop model-based approaches for variable rate nitrogen fertilization in winter wheat. Precis. Agric. 23, 1922–1948. https://doi.org/10.1007/s11119-022-09957-5.

Grant, C.A., Wu, R., Selles, F., Harker, K.N., Clayton, G.W., Bittman, S., Zebarth, B.J., Lupwayi, N.Z., 2012. Crop yield and nitrogen concentration with controlled release urea and split applications of nitrogen as compared to non-coated urea applied at seeding. Field Crop. Res. 127, 170–180. https://doi.org/10.1016/j.fcr.2011.11.002.

Hawkesford, M.J., 2014. Reducing the reliance on nitrogen fertilizer for wheat production. J. Cereal Sci. 59, 276–283. https://doi.org/10.1016/j.jcs.2013.12.001.

Hawkesford, M.J., Riche, A.B., 2020. Impacts of G x E x M on nitrogen use efficiency in wheat and future prospects. Front. Plant Sci. 11, 1157. https://doi.org/10.3389/fpls.2020.01157.

Hellemans, T., Landschoot, S., Dewitte, K., Van Bockstaele, F., Vermeir, P., Eeckhout, M., Haesaert, G., 2018. Impact of crop husbandry practices and environmental conditions on wheat composition and quality: a review. J. Agric. Food Chem. 66, 2491–2509. https://doi.org/10.1021/acs.jafc.7b05450.

Hirel, B., Le Gouis, J., Ney, B., Gallais, A., 2007. The challenge of improving nitrogen use efficiency in crop plants: towards a more central role for genetic variability and quantitative genetics within integrated approaches. J. Exp. Bot. 58, 2369–2387. https://doi.org/10.1093/jxb/erm097.

Hoefsloot, P., Ines, A., Dam, J.C., Duveiller, G., Kayitakire, F., Hansen, J., 2012. Combining Crop Models and Remote Sensing for Yield Prediction: Concepts, Applications and Challenges for Heterogeneous Smallholder Environments. Report of CCFAS-JRC Workshop at Joint Research Centre, Ispra, Italy, June 13-14, 2012. ⟨https://publications.jrc.ec.europa.eu/repository/bitstream/JRC77375/lbna25643enn.pdf⟩ (Accessed October 10, 2023). 1831-9424.

Holland, K.H., Schepers, J.S., 2010. Derivation of a variable rate nitrogen application model for in-season fertilization of corn. Agron. J. 102 (5), 1415–1424. https://doi.org/10.2134/agronj2010.0015.

Jiang, J., Wang, C., Wang, Y., Cao, Q., Tian, Y., Zhu, Y., Cao, W., Liu, X., 2020. Using an active sensor to develop new critical nitrogen dilution curve for winter wheat. Sensors 20, 1577. https://doi.org/10.3390/s20061577.

Kaliraj, S., Srinivas, R., Kiruthika, N., Vairaveni, E., Mohamed, H., Palanivel, K., Lakshumanan, C., Chandrasekar, N., 2024. Chapter 4 -Remote sensing indices based soil properties measurement – a case study of the Thamirabarani River Basin, South India. In: Dharumarajan, S., Kaliraj, S., Adhikari, K., Lalitha, M., Kumar, N. (Eds.), Remote Sensing of Soils, Chapter 4. Elsevier, pp. 45–63. https://doi.org/10.1016/B978-0-443-18773-5.00030-2.

Landolfi, V., Visioli, G., Blandino, M., 2021. Effect of nitrogen fertilization and fungicide application at heading on the gluten protein composition and rheological quality of wheat. Agronomy 11, 1687. https://doi.org/10.3390/agronomy11091687.

Li, F., Miao, Y., Hennig, S.D., Gnyp, M.L., Chen, X., Jia, L., Bareth, G., 2010. Evaluating hyperspectral vegetation indices for estimating nitrogen concentration of winter wheat at different growth stages. Precis. Agric. 11 (4), 335–357. https://doi.org/10.1007/s11119-010-9165-6.

Litke, L., Gaile, L., Ruža, A, Z., 2018. Effect of nitrogen fertilization on winter wheat yield and yield quality. Agron. Res. 16, 500–509. ⟨https://doi.org/10.15159/AR.18.064⟩.

Ma, Q., Wang, M., Zheng, G., Yao, Y., Tao, R., Zhu, M., Ding, J., Li, C., Guo, W., Zhu, X., 2021. Twice-split application of controlled-release nitrogen fertilizer met the nitrogen demand of winter wheat. Field Crop. Res. 267, 108163 https://doi.org/10.1016/j.fcr.2021.108163.

Malhi, S.S., Grant, C.A., Johnston, A.M., Gill, K.S., 2001. Nitrogen fertilization management for no-till cereal production in the Canadian Great Plains: a review. Soil Tillage Res 60, 101–122. https://doi.org/10.1016/S0167-1987(01)00176-3.

Marinaccio, F., Blandino, M., Reyneri, A., 2016. Effect of nitrogen fertilization on yield and quality of durum wheat cultivated in northern Italy and their interaction with different soils and growing seasons. J. Plant Nutr. 39, 643–654. https://doi.org/10.1080/01904167.2015.1087027.

Marino, S., Tognetti, R., Alvino, A., 2011. Effects of varying nitrogen fertilization on crop yield and grain quality of emmer grown in a typical Mediterranean environment in central Italy. Eur. J. Agron. 34, 172–180. https://doi.org/10.1016/j.eja.2010.10.006.

Mezera, J., Lukas, V., Horniaček, I., Smutný, V., Elbl, J., 2021. Comparison of proximal and remote sensing for the diagnosis of crop status in site-specific crop management. Sensors 22, 19. https://doi.org/10.3390/s22010019.

Montemurro, F., 2009. Different Nitrogen Fertilization Sources, Soil Tillage, and Crop Rotations in Winter Wheat: Effect on Yield, Quality, and Nitrogen Utilization. J. Plant Nutr. 32, 1–18. https://doi.org/10.1080/01904160802530979.

Morlin Carneiro, F., Angeli Furlani, C.E., Zerbato, C., Candida De Menezes, P., Da Silva Gírio, L.A., Freire De Oliveira, M., 2020. Comparison between vegetation indices for detecting spatial and temporal variabilities in soybean crop using canopy sensors. Precis. Agric. 21 (5), 979–1007. https://doi.org/10.1007/s11119-019-09704-3.

Mulla, D.J., 2013. Twenty-five years of remote sensing in precision agriculture: Key advances and remaining knowledge gaps. Biosyst. Eng. 114 (4), 358–371. https://doi.org/10.1016/j.biosystemseng.2012.08.009.

Ortuzar-Iragorri, M.A., Aizpurua, A., Castellón, A., Alonso, A., Estavillo, J.M., Besga, G., 2018. Use of an N-tester chlorophyll meter to tune a late third nitrogen application to wheat under humid Mediterranean conditions. J. Plant Nutr. 41 (5), 627–635. https://doi.org/10.1080/01904167.2017.1414243.

Pennacchi, J.P., Virlet, N., Barbosa, J.P.R.A.D., Parry, M.A.J., Feuerhelm, D., Hawkesford, M.J., Carmo-Silva, E., 2022. A predictive model of wheat grain yield based on canopy reflectance indices and theoretical definition of yield potential. Theor. Exp. Plant Physiol. 34, 537–550. https://doi.org/10.1007/s40626-022-00263-z.

Prey, L., Schmidhalter, U., 2019. Temporal and spectral optimization of vegetation indices for estimating grain nitrogen uptake and late-seasonal nitrogen traits in wheat. Sensors 19, 4640. https://doi.org/10.3390/s19214640.

Prystupa, P., Slafer, G.A., Savin, R., 2003. Leaf appearance, tillering and their coordination in response to NxP fertilization in barley. Plant Soil 255 (2), 587–594. https://doi.org/10.1023/A:1026018702317.

Quebrajo, L., Pérez-Ruiz, M., Rodriguez-Lizana, A., Agüera, J., 2015. An approach to precise nitrogen management using hand-held crop sensor measurements and winter wheat yield mapping in a mediterranean environment. Sensors 15 (3), 5504–5517. https://doi.org/10.3390/s150305504.

Raun, W.R., Solie, J.B., Johnson, G.V., Stone, M.L., Lukina, E.V., Thomason, W.E., Schepers, J.S., 2001. In-season prediction of potential grain yield in winter wheat using canopy reflectance. Agron. J. 93 (1), 131–138. https://doi.org/10.2134/agronj2001.931131.

Samborski, S.M., Tremblay, N., Fallon, E., 2009. Strategies to make use of plant sensors-based diagnostic information for nitrogen recommendations. Agron. J. 101 (4), 800–816. https://doi.org/10.2134/agronj2008.0162Rx.

Schulz, R., Makary, T., Hubert, S., Hartung, K., Gruber, S., Donath, S., Döhler, J., WEIß, K., Ehrhart, E., Claupein, W., Piepho, H.-P., Pekrun, C., Müller, T., 2015. Is it necessary to split nitrogen fertilization for winter wheat? On-farm research on Luvisols in South-West Germany. J. Agric. Sci. 153, 575–587. https://doi.org/10.1017/S0021859614000288.

Sieling, K., Kage, H., 2021. Apparent fertilizer N recovery and the relationship between grain yield and grain protein concentration of different winter wheat varieties in a long-term field trial. Eur. J. Agron. 124, 126246. https://doi.org/10.1016/j.eja.2021.126246.

Tabak, M., Lepiarczyk, A., Filipek-Mazur, B., Lisowska, A., 2020. Efficiency of Nitrogen Fertilization of Winter Wheat Depending on Sulfur Fertilization. Agronomy 10, 1304. https://doi.org/10.3390/agronomy10091304.

Tremblay, N., Fallon, E., Ziadi, N., 2011. Sensing of Crop Nitrogen Status: Opportunities, Tools, Limitations, and Supporting Information Requirements. HortTechnology 21 (3), 274–281. https://doi.org/10.21273/HORTTECH.21.3.274.

Tucker, C.J., Townshend, J R.G., Goff, T.E., 1985. African Land-Cover Classification Using Satellite Data. Science 227 (4685), 369–375. https://doi.org/10.1126/science.227.4685.369.

Vannoppen, A., Gobin, A., Kotova, L., Top, S., De Cruz, L., Vīksna, A., Aniskevich, S., Bobylev, L., Buntemeyer, L., Caluwaerts, S., De Troch, R., Gnatiuk, N., Hamdi, R., Reca Remedio, A., Sakalli, A., Van De Vyver, H., Van Schaeybroeck, B., Termonia, P., 2020. Wheat yield estimation from NDVI and regional climate models in Latvia. Remote Sens 12, 2206. https://doi.org/10.3390/rs12142206.

Wang, K., Huggins, D.R., Tao, H., 2019. Rapid mapping of winter wheat yield, protein, and nitrogen uptake using remote and proximal sensing. Int. J. Appl Earth Obs. 82, 101921. https://doi.org/10.1016/j.jag.2019.101921.

Wang, W., Yao, X., Tian, Y., Liu, X., Ni, J., Cao, W., Zhu, Y., 2012. Common Spectral Bands and Optimum Vegetation Indices for Monitoring Leaf Nitrogen Accumulation in Rice and Wheat. J. Integr. Agric. 11, 2001–2012. https://doi.org/10.1016/S2095-3119(12)60457-2.

Zadoks, J.C., Chang, T.T., Konzak, C.F., 1974. A decimal code for the growth stages of cereals. Weed Res 14, 415–421. https://doi.org/10.1111/j.1365-3180.1974.tb01084.x.

Zhang, J., Hu, Y., Li, F., Fue, K.G., Yu, K., 2024. Meta-Analysis Assessing Potential of Drone Remote Sensing in Estimating Plant Traits Related to Nitrogen Use Efficiency. Remote Sens. 16 (5), 838. https://doi.org/10.3390/rs16050838.

Zhang, Z., Yu, Z., Zhang, Y., Shi, Y., 2021. Split nitrogen fertilizer application improved grain yield in winter wheat (*Triticum aestivum* L.) via modulating antioxidant capacity and 13C photosynthate mobilization under water-saving irrigation conditions. Ecol. Process 10, 21. https://doi.org/10.1186/s13717-021-00290-9.

Zhao, B., Duan, A., Ata-Ul-Karim, S.T., Liu, Zhandong, Chen, Z., Gong, Z., Zhang, J., Xiao, J., Liu, Zugui, Qin, A., Ning, D., 2018. Exploring new spectral bands and vegetation indices for estimating nitrogen nutrition index of summer maize. Eur. J. Agron. 93, 113–125. https://doi.org/10.1016/j.eja.2017.12.006.